Fermi National Accelerator Laboratory

FERMILAB-Conf-93/127

Electroweak Results from DØ

Marcel Demarteau
for the DØ Collaboration

Fermi National Accelerator Laboratory
P.O. Box 500, Batavia, Illinois 60510

May 1993

Presented at the *XXVIIIth Rencontres de Moriond, Electroweak Interactions and Unified Theories*, Les Arcs, Bourg Saint Maurice, France, March 13-20, 1993

Disclaimer

Electroweak Results from DØ

Marcel Demarteau
Fermilab
Batavia, IL 60510

Representing the DØ collaboration*

Abstract

Preliminary results from DØ are presented on properties of the $W^{\pm}$ and Z^0 electroweak gauge bosons, using final states containing electrons and muons. In particular, preliminary measurements of the $W^{\pm}$ and Z^0 production cross sections with decay into final states containing electrons are shown and a status report on the determination of M_W/M_Z is given.

*Universidad de los Andes (Colombia), University of Arizona, Brookhaven National Laboratory, Brown University, University of California, Riverside, Centro Brasiliero de Pesquisas Fisicas (Brazil), CINVESTAV (Mexico), Columbia University, Delhi University (India), Fermilab, Florida State University, University of Hawaii, University of Illinois, Chicago, Indiana University, Iowa State University, Korea University (Korea), Lawrence Berkeley Laboratory, University of Maryland, University of Michigan, Michigan State University, Moscow State University (Russia), New York University, Northeastern University, Northern Illinois University, Northwestern University, University of Notre Dame, Panjab University (India), Institute for High Energy Physics (Russia), Purdue University, Rice University, University of Rochester, CEN Saclay (France), State University of New York, Stony Brook, SSC Laboratory, Tata Institute of Fundamental Research (India), University of Texas, Arlington, Texas A&M University

1 Introduction

DØ is a large multi-purpose detector operating at the Tevatron $\overline{p}p$ Collider, located at Fermi National Accelerator Laboratory. It features a non-magnetic inner tracking system, compact, hermetic calorimetry for the detection of electrons, jets and missing transverse energy, and an extensive muon system. The DØ detector has been described in detail elsewhere [1]; here only the features relevant for the analyses described below will be discussed briefly.

The inner tracking region covers a cylindrical region of radius 75 cm and 3 m in length with wire gas drift chamber detectors to detect charged tracks in a pseudorapidity range of $|\eta| < 3$ with full azimuthal coverage. An additional three layer cylindrical transition radiation detector helps with the electron identification over a range $|\eta| < 1.2$.

The calorimeter is a uranium–liquid argon sampling detector, contained within a central cryostat and two end cryostats which provide coverage over the range $|\eta| < 4.2$. The electromagnetic section is 21 X_0 deep and has a fractional energy resolution of $15\%/\sqrt{E}$, where E is in GeV, while the hadronic section is 7 - 9 interaction lengths (λ) thick and has a measured fractional energy resolution for pions of $50\%/\sqrt{E}$ [2].

The muon system is located outside the calorimeter cryostats. It consists of three layers of chambers, with magnetized iron toroids located between the first and second layers. Each layer has 3 or 4 planes of proportional wire drift tubes. The magnetic field in the iron toroid is 1.9 Tesla, providing momentum measurement with a design resolution of $\sigma(p)/p = 0.2 \oplus 0.001p$ as well as charge discrimination up to 350 GeV/c. The thickness of the calorimeter plus iron toroids varies from 14 λ in the central region to 19 λ in the forward region.

The DØ detector was commissioned with $\overline{p}p$ collisions during the summer of 1992 and began taking data in August, 1992. At the time of this conference, over 8 pb^{-1} of data have been logged. The results presented here are preliminary, and based on only part of the data accumulated to date. The total data sample is anticipated to be in excess of 15 pb^{-1} by the end of the run in June, 1993.

2 $W^{\pm}$ and Z^0 Decays to Muons

$W^{\pm}$ and Z^0 decays to muons are triggered with a 3 level trigger. At Level 1, a fast hardware trigger requires at least 2 of 3 muon layers to have hits within a wide road, which effectively requires the transverse momentum to exceed 5 GeV/c. For single and di-muon events the trigger is limited to the pseudo-rapidity region $|\eta| < 1.7$. A Level 1.5 trigger requires all three layers to have hits within a smaller road, imposing a minimum p_t threshold of 7 GeV/c. Finally, the Level 2 software trigger imposes cuts similar to those performed off-line, requiring a single muon with $p_t > 15$ GeV/c for W-candidate events or two muons each with $p_t > 10$ GeV/c for Z^0-candidates. Also cosmic rejection cuts are applied at this trigger level.

Off-line, additional track quality cuts are applied for the muon identification. The muon track is required to have hits in the chamber before the magnet, and the residuals have to be less than 1 cm and 7 cm for the bend and non-bend view, respectively. Furthermore, the track is required to have a vertex impact parameter for the non-bend view of $\delta(xy) < 10$ cm and $\delta(Rz) < 25$ cm for the bend view and a matching central detector track with $|\Delta\vartheta| < 0.3$ rad and $|\Delta\varphi| < 0.25$ rad. Additional requirements include

a matching minimum-ionizing energy deposition in the calorimeter, and an isolation cut on calorimeter activity near the muon track. To remove poorly measured muons in the transition region between the central and end toroids, a minimum path-length through the magnetized iron toroid of $\int Bdl > 2.0\ Tm$, corresponding to a p_t kick of 0.6 GeV/c, is required.

For $W^{\pm} \rightarrow \mu^{\pm}\nu$ events, a muon with $p_t > 20\ GeV/c$ is required together with missing transverse momentum greater than 20 GeV/c. $Z^0 \rightarrow \mu^+\mu^-$ events are selected by requiring one muon with $p_t > 20\ GeV/c$ and a second muon with $p_t > 15\ GeV/c$. For cosmic rejection, there are the additional requirements that the muons must not be back-to-back, *i.e.* $\Delta\varphi < 160°$ or $\Delta\vartheta < 170°$. This event selection yielded 1166 $W^{\pm}$ and 33 Z^0-candidate events in an integrated luminosity of 4 pb^{-1} with a negligible background in the Z^0 sample. The background in the W-sample is still under study and is expected to be brought to a level of less than 10%.

3 W and Z Decays to Electrons

3.1 Electron Identification

The offline electron identification requirements are common to both the cross section and mass analyses, so they are presented here. There are essentially four quantities of an electromagnetic energy cluster that are used in the electron identification: *i)* fraction of electromagnetic energy, *ii)* shower shape χ^2, *iii)* isolation and *iv)* track match significance.

Since very little leakage out of the 21 X_0 thick electromagnetic calorimeter section is expected, the first condition simply requires the ratio of the electromagnetic energy over the total energy of the cluster to be greater than 0.9. To ensure that both the longitudinal and transverse shape of the shower are consistent with an electron, an energy covariance matrix technique is used [3]. In this technique a training sample of electrons is used to compute the covariance matrix of the energies deposited in each calorimeter element. This is done as a function of energy and pseudo-rapidity. Using the inverse of this correlation matrix (the "H-matrix") a χ^2-like variable is constructed based on the observed energy depositions in the calorimeter, which is then cut on to discriminate against background. The isolation variable, the third quantity used in the electron identification, is defined as the ratio $(E(0.4) - EM(0.2))/EM(0.2)$. Here $E(0.4)$ is the total energy inside a cone around the center of the electromagnetic cluster defined by $\sqrt{\Delta\eta^2 + \Delta\varphi^2} < 0.4$; $EM(0.2)$ is the electromagnetic energy in a cone of radius 0.2. The isolation was required to be less than 0.15. Finally, a good match between the reconstructed track in the central detector and the shower position in the calorimeter was required. The track match significance variable, defined as $\sqrt{(R\,\Delta\varphi/\sigma(R\,\Delta\varphi))^2 + (\Delta z/\sigma(\Delta z))^2)}$, was required to be less than 10.

3.2 $W^{\pm}$ and Z^0 Production Cross Section

A preliminary measurement of the production cross sections for $W^{\pm} \rightarrow e^{\pm}\nu_e$ and $Z^0 \rightarrow e^+e^-$ was performed using an event sample based on an integrated luminosity of 3.45 pb^{-1}. W-candidate events were selected by requiring an electron with transverse energy and missing transverse energy greater than 25 GeV. For Z^0-events two electrons with $E_t > 25\ GeV$ were required. The electrons must be well within the acceptance of the electromagnetic calorimeter, which is defined here as $|\eta| < 1.1$ or $1.5 < |\eta| < 3.2$. Also

the regions in the central calorimeter which are near the small azimuthal gaps between calorimeter modules where the response is slightly degraded were excluded. These gaps occur every 0.2 radians, and the measured electron position was required to be at least 0.01 radians away, resulting in a 10% loss in efficiency. The combined efficiency for these kinematic and fiducial requirements is 0.51 ± 0.04 for W's and 0.42 ± 0.04 for Z's.

The $W^{\pm}$ and Z^0 events were required to satisfy the same trigger. In the Level 1 trigger the events had to pass a 10 GeV threshold for one electromagnetic trigger tower ($\Delta\eta \times \Delta\varphi = 0.2 \times 0.2$). In Level 2 one electron with $E_t > 20$ GeV was required which also passed shower shape and isolation cuts. The trigger efficiency was determined using diagnostic triggers which had a lower E_t requirement or did not impose electron shape and isolation requirements. The trigger efficiency for events which satisfied the kinematic and fiducial requirements described above was measured to be 0.92 ± 0.03 for W's and 0.99 ± 0.01 for Z's.

Finally, the electrons had to satisfy basically the four standard electron identification requirements described in section 3.1. The combined efficiency of the electron identification cuts for a single electron from W decays was 0.68 ± 0.05, and for both electrons from Z^0 decays the efficiency was 0.46 ± 0.07. The greatest source of inefficiency at this time is the track match requirement which will improve when detector calibration and alignment studies are complete. The combined efficiency for all selection criteria is 0.32 ± 0.03 for W's and 0.19 ± 0.03 for Z's.

These criteria, applied to a data set of 3.45 ± 0.41 pb^{-1}, yielded a total of 2824 $W^{\pm} \rightarrow e^{\pm}\nu_e$ and 172 $Z^0 \rightarrow e^+e^-$ candidates. The backgrounds in the W-sample were estimated to be $(1.0 \pm 0.4)\%$ from $W^{\pm} \rightarrow \tau^{\pm}\nu_{\tau}$ followed by $\tau^{\pm} \rightarrow e^{\pm}\nu_{\tau}\nu_e$, $(1.6 \pm 1)\%$ from QCD 2-jet events, and $(1.0 \pm 0.5)\%$ from $Z^0 \rightarrow e^+e^-$ events where one electron was lost. The total background in the W-sample was $(3.6 \pm 1.2)\%$. For Z^0's a fit was performed to the data using the sidebands to estimate the background under the peak. The result was a background estimate of $(10 \pm 3)\%$.

Correcting the event yields for the estimated background levels and for inefficiencies due to detector acceptance and event selection criteria, the results for the production rates are:

$$\begin{aligned} \sigma(p\bar{p} \rightarrow W^{\pm}) \cdot BR(W^{\pm} \rightarrow e^{\pm}\nu_e) &= 2.48 \pm 0.05 \pm 0.26 \pm 0.30 \; nb \\ \sigma(p\bar{p} \rightarrow Z^0) \cdot BR(Z^0 \rightarrow e^+e^-) &= 0.235 \pm 0.019 \pm 0.040 \pm 0.028 \; nb \end{aligned}$$

The quoted errors are statistical, systematic, and due to the error in the luminosity, respectively. The systematic error includes the uncertainty due to structure functions. The Z^0 cross section is corrected for the virtual photon terms. At present the errors are dominated by the systematic errors in the efficiency calculations and in the luminosity determination, but significant improvements are expected in both as the analyses mature.

The ratio of the above rates is interesting because many common sources of error cancel, including all of the error on the luminosity and part of the errors on the acceptance and event selection efficiency. The ratio can be related to $\Gamma(W)$ in the following way:

$$R \equiv \frac{\sigma \cdot BR(W^{\pm} \rightarrow e^{\pm}\nu_e)}{\sigma \cdot BR(Z^0 \rightarrow e^+e^-)} = \frac{\Gamma(W^{\pm} \rightarrow e^{\pm}\nu_e)}{\Gamma(W)} \frac{\Gamma(Z)}{\Gamma(Z^0 \rightarrow e^+e^-)} \frac{\sigma(p\bar{p} \rightarrow W^{\pm})}{\sigma(p\bar{p} \rightarrow Z^0)} \qquad (1)$$

From the results quoted above one obtains $R = 10.55 \pm 0.87 \pm 1.07$. This yields a measurement of the width of the W-boson using the known values for the other factors

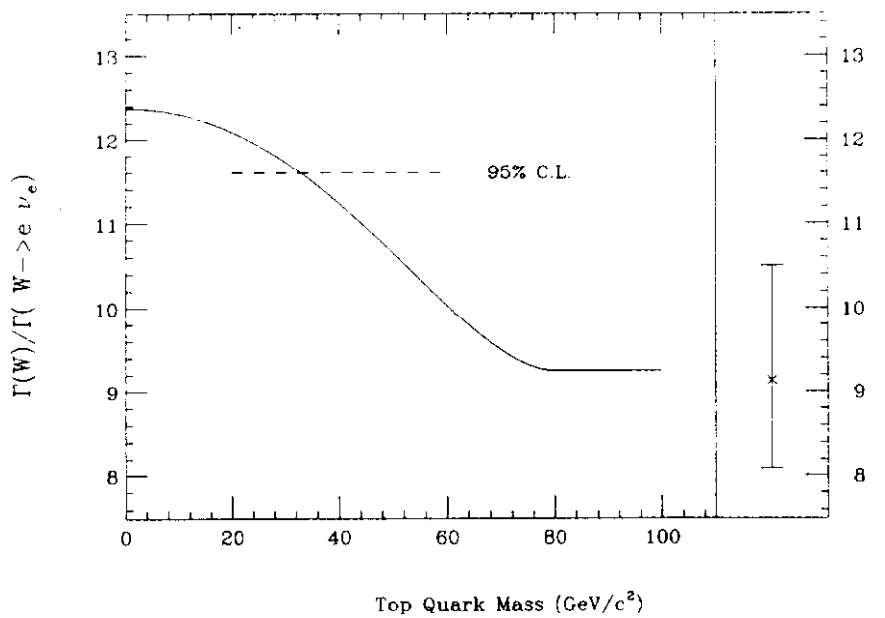

Figure 1: The ratio $\Gamma(W)/\Gamma(W^{\pm} \rightarrow e^{\pm}\nu)$ as a function of M_t, together with the preliminary DØ measurement and the 95% C.L. limit.

in the equation. Using for the Z^0 width the value measured by the LEP-experiments, $\Gamma(Z^0) = 2.487 \pm 0.010\ GeV$ [4] and the theoretical value for both the ratio of $W^{\pm}$ to Z^0 production cross section, $\sigma(p\bar{p} \rightarrow W^{\pm})/\sigma(p\bar{p} \rightarrow Z^0) = 3.23 \pm 0.03$ [5] and the ratio of $W^{\pm}$ and Z^0 electron decay widths, $\Gamma(W^{\pm} \rightarrow e\nu_e)/\Gamma(Z^0 \rightarrow e^+e^-)) = 2.70 \pm 0.02$ [6], one obtains, using equation 1, a value for the total decay width of the W-boson of $\Gamma(W) = 2.06 \pm 0.27\ GeV$.

This meaurement of $\Gamma(W)$ can be used to set a limit on non-standard decay modes of the W. In particular, this result can be used to set a limit on the top quark mass which is independent of the top decay modes. In Figure 1 the ratio $\Gamma(W)/\Gamma(W^{\pm} \rightarrow e^{\pm}\nu_e)$ is plotted as a function of top quark mass, together with the preliminary DØ result $\Gamma(W)/\Gamma(W^{\pm} \rightarrow e^{\pm}\nu_e) = 9.2^{+1.4}_{-1.1}$. The LEP value for $\Gamma(Z^0 \rightarrow e^+e^-)$ of $83.20 \pm 0.55\ MeV$ [4] has been used in obtaining this result. The 95% C.L. upper limit on $\Gamma(W)/\Gamma(W^{\pm} \rightarrow e^{\pm}\nu_e)$ is 11.6, corresponding to a lower top quark mass limit of $M_t > 33\ GeV/c^2$.

3.3 $W^{\pm}$ and Z^0 Mass

A slightly different data sample was used for the measurement of the W and Z^0 masses. The selection was based on "Express Line" data, a small subset of triggers, rich in events of high interest, which are written directly to disk and immediately analyzed. The trigger requirement for Express Line W-candidates was, at the first level trigger, one electromagnetic trigger tower with $E_t > 10\ GeV$. For Z^0 candidates two electromagnetic trigger towers with $E_t > 7\ GeV$ were required. At the Level 2 trigger the W-candidates were required to have one electromagnetic cluster with $E_t > 20\ GeV$ and missing transverse energy of at least 20 GeV. The electron candidate was also required to pass the Level 2 software electron filter, which imposed shower shape and isolation requirements. For Z^0 candidates, two electrons were required passing the Level 2 shower-shape and isolation cuts, each with $E_t > 20\ GeV$.

At the offline stage the same electron identification cuts were applied as described above in section 3.1. The kinematic requirements of the Level 2 trigger were again im-

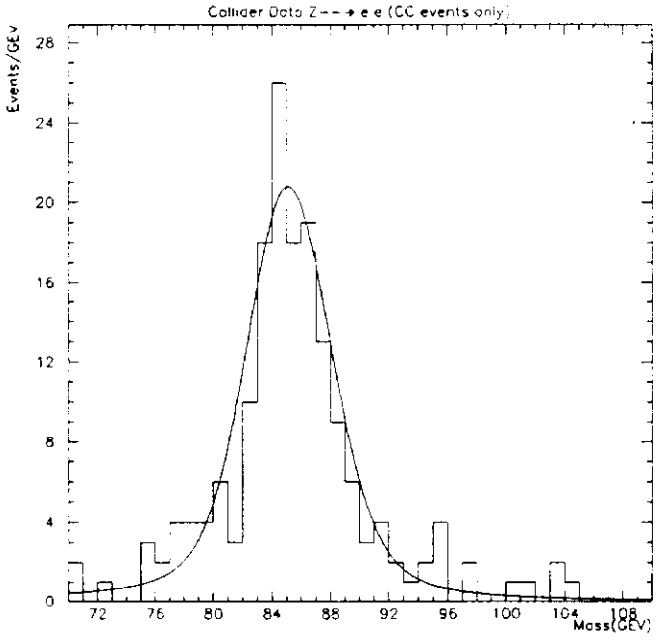

Figure 2: Di-electron invariant mass distribution for Z-candidate events with both electron legs in the central calorimeter.

posed using the offline clustering algorithm, which differs from the Level 2 algorithm. In addition, W-candidates were required to satisfy $p_t(W) < 30\ GeV/c$. In order to limit the systematic uncertainties in the determination of the masses due to the energy scale, the data samples were restricted to the central calorimeter only. That is, the single electron in W-events and both electrons in Z^0-events were required to lie within a pseudo-rapidity range $|\eta| \leq 1.1$. Moreover, electrons within .01 radians of the azimuthal boundaries between electromagnetic calorimeter modules were removed. This event selection yielded 170 Z^0-candidates and 2904 W-candidates in an integrated luminosity of $\mathcal{L} = 6.0 \pm 0.7\ pb^{-1}$.

The mass of the Z^0 is determined by performing an unbinned maximum likelihood fit on the di-electron invariant mass distribution. The invariant mass distribution is fit to a likelihood distribution of the form:

$$f(m_i, \sigma_i, M_Z, \Gamma_Z) \quad = \int_0^\infty \frac{e^{-\beta m'}\, m'^2}{(m'^2 - M_Z^2)^2 + \frac{m'^4 \Gamma_Z^2}{M_Z^2}} \; \frac{1}{\sqrt{2\pi}\,\sigma_i}\, e^{-\frac{(m'-m_i)^2}{2\sigma_i^2}}\, dm'$$

This is a convolution of the parton luminosity distribution, characterized by the parameter β, and a relativistic Breit-Wigner folded with a Gaussian detector resolution. The width of the Z^0 was fixed in the fit to $\Gamma_Z = 2.5\ GeV$. The parameter β was taken to be 0.015 as determined from the ISAJET Monte Carlo. Figure 2 shows the di-electron invariant mass distribution for the central calorimeter Z^0-sample. The fitted mass value is 85.2 GeV/c^2, considerably lower than the LEP Z-mass. The question of the absolute energy calibration in DØ will be addressed below.

The W-mass is extracted from the transverse mass distribution, where transverse mass is defined as the invariant mass of the electron and neutrino in the transverse plane

$$M_T \quad = \sqrt{2\, E_T^e\, E_T^\nu\, (1 - cos\varphi^{e\nu})}$$

Here the angle $\varphi^{e\nu}$ is the azimuthal angle between the electron and the neutrino. The

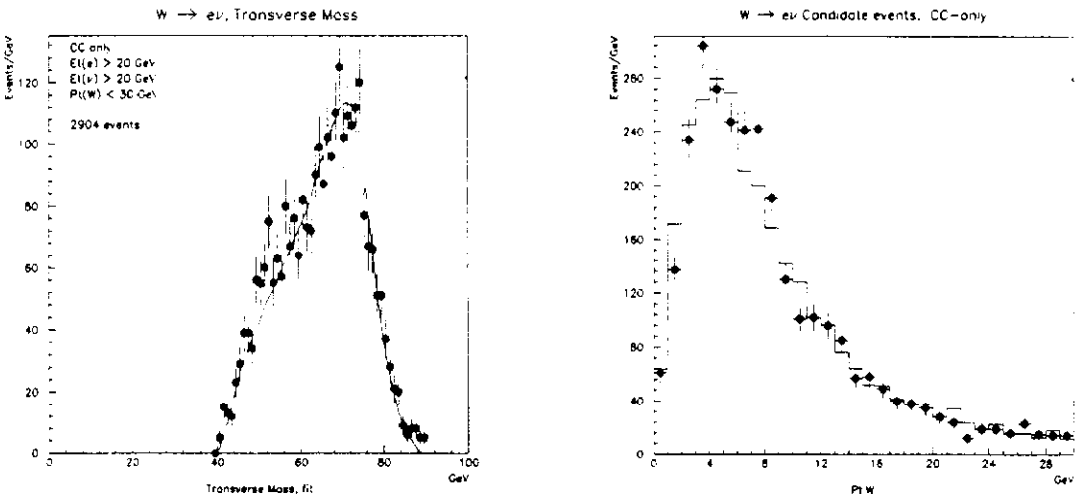

Figure 3: Distribution of the transverse mass (a) and the W transverse momentum of $W^{\pm} \rightarrow e^{\pm}\nu_e$ events. The points are the data; the solid line is the fit.

transverse mass distribution is compared to Monte Carlo distributions generated for different W-masses taking into account detector effects. The generation of the Monte Carlo events is done in several steps. First, the W-boson momentum vector is generated according to the longitudinal and transverse momentum distributions of Arnold and Kauffmann [7]. A mass is generated according to a relativistic Breit-Wigner line-shape, the W is decayed in its center of mass, taking into account its angular distribution, and the decay particles are boosted to the lab-frame. Both electron decays and $\tau \rightarrow e\nu_e\nu_\tau$ decays of the W are taken into account.

The second step in the generation of the W events is a fast simulation of the DØ detector. One of the important features of this detector model is that the underlying event is simulated using real minimum bias data. For the results presented here, the underlying event for a W decay has been simulated with a single minimum bias event. It should be noted that, as the Tevatron luminosity increases, it becomes increasingly important to take into account the effect of multiple interactions, so this model will be refined in the future. After the underlying event is superimposed on the W-event, the $\not\!\!E_t$ is recalculated and the electron energy and hadronic recoil are smeared according to the resolution as measured in the testbeam and DØ. In the simulation, the hadronic recoil of the W is scaled down by 24% to agree with the results obtained from studies of $\vec{p}_t$ balance in Z^0 events. In the final stage of the event generation the various efficiencies and fiducial cuts are modelled, the most important being the different tracking efficiencies for the central and forward regions.

The Monte Carlo events are generated in a grid of 21 W-masses around a central value in steps of 400 MeV in mass with 10^6 events per mass point. A binned maximum likelihood fit of the Monte Carlo to the transverse mass distribution of the data is then performed in a mass window of 40-90 GeV/c^2. Figure 3 shows the transverse mass distribution (a) and the $p_t(W)$ spectrum (b), with the fit results superimposed. The Monte Carlo fit agrees well with the data, demonstrating that the calorimeter response is well understood and modelled. It should be noted that it is the ratio M_W/M_Z which is of interest, since M_Z has been very precisely determined by LEP and SLC. In this ratio the overall energy scale partly cancels out. From these preliminary data a value of M_W/M_Z

is obtained which is in agreement with the world average, indicating that the low value for the Z^0-mass, quoted above, is more likely the result of an error in energy scale than an offset error. However, this issue requires more study, and we postpone quoting a value for the ratio M_W/M_Z until we can properly assign the error in this ratio which results from our energy scale uncertainty. The energy scale of the calorimeter is under close investigation within the collaboration, and when it has been understood we are confident that we will make a very competitive measurement of the W mass.

4 Acknowledgements

I would like to thank the organizers of the conference for an exciting conference in a very pleasant atmosphere.

References

[1] S. Abachi, *et. al.*, to be submitted to NIM.

[2] S. Abachi, *et. al.*, Nucl. Instr. Meth. **A324** 53 (1993).

[3] R. Engelmann *et.al.*, Nucl. Instr. Meth **216** 45 (1983)
M. Narain, "Proceedings of the annual meeting of the Division of Particles and Fields of the American Physical Society", Fermilab, Batavia, IL, Nov (1992).

[4] The LEP collaborations: ALEPH, DELPHI, L3 and OPAL. Phys. Lett. **B276**, 247 (1992).

[5] A.D.Martin,W.J. Stirling, and R.G. Roberts, Phys. Lett. **B228**, 149 (1989).

[6] W.F.L. Hollik, Fortschr. Phys. **38**, 165 (1990).

[7] P. B. Arnold and R. P. Kauffmann, Nuc. Phys. **B349** 381 (1991).